Received: 21 November 2019 | Revised: 22 January 2020 | Accepted: 6 March 2020

DOI: 10.1002/rcm.8777

RESEARCH ARTICLE

Rapid Communications in Mass Spectrometry WILEY

Mass spectral fragmentation of perfluoroacyl derivatives of half nitrogen mustards for their detection by gas chromatography/mass spectrometry

Buddhadeb Chandra | Kanchan Sinha Roy | Mahabul Shaik | Chandrakant Waghmare | Meehir Palit

VERTOX – Biochemistry Division, Defence Research and Development Establishment, Jhansi Road, Gwalior 474002, Madhya Pradesh, India

Correspondence
M. Palit, VERTOX – Biochemistry Division, Defence Research and Development Establishment, Jhansi Road, Gwalior-474002, Madhya Pradesh, India.
Email: meehirpalit@rediffmail.com

Rationale: Analytical methods for the detection and identification of half nitrogen mustards (halfNMs), i.e., partially hydrolyzed products of nitrogen mustards (pHpNMs), using silyl derivatives are often associated with low sensitivity and selectivity. In order to overcome these limitations, the derivatization of halfNMs was performed using perfluoroacylation.

Methods: Two efficient derivatization techniques using trifluoroacetyl (TFA) and heptafluorobutyryl (HFB) groups were developed for the unambiguous identification of halfNMs. A mass spectral database was generated by performing gas chromatography/electron ionization mass spectrometry (GC/EI-MS) and gas chromatography/positive chemical ionization mass spectrometry (GC/PCI-MS). The fragmentation pathways were studied by tandem mass spectrometry (MS/MS) in both EI and PCI mode.

Results: The EI-MS spectra of the TFA and HFB derivatives of halfNMs contain intense molecular ions and fragment ions, thus making perfluoroacylation preferable to silylation. In addition, the background-free chromatogram obtained using these derivatives provides unambiguous identification of these compounds in blind samples. The structures of the fragment ions were postulated, and the sources of significant ions were traced by performing MS/MS precursor ion scans. In the PCI-MS spectra, along with the protonated molecule, significant peaks due to neutral losses of HF, HCl, CH_3Cl and CF_3COOH were observed.

Conclusions: This is the first report of the elucidation of the fragmentation pathways of perfluoroacyl derivatives of halfNMs. The complementary GC/PCI-MS and GC/PCI-MS/MS data will be helpful in the identification of unknown metabolites in a fast and reliable fashion.

1 | INTRODUCTION

Nitrogen mustards (NMs) are schedule 1 chemical warfare agents (CWAs)[1] in the Chemical Weapon Convention (CWC).[2] These agents are highly toxic with strong vesicant properties that corrode mucosal membranes as well as causing skin and eye damage, affect the respiratory system and lead to failure of internal organs.[3] In addition to the formation of painful blisters, these vesicant agents can alkylate DNA[4] and free nucleophilic sites present in proteins,[5] leading to cancer and metabolic disorders. Such CWAs remain a high-priority concern due to the their possible use against civilian targets, as occurred in the 1995 subway attack with sarin in Tokyo.[6] As mustard

agents are easier to synthesize and deploy than nerve agents, the development of analytical methods for their detection, and for the study of their toxicology and metabolism, is necessary for public safety. Although there is much literature available on sulfur mustards, there is very little on biomarkers for NMs, because NMs have not been used in a real-life scenario. However, the possibility of their deployment cannot be ignored. In this investigation we have focused on the derivatization and mass spectral identification of half nitrogen mustards (halfNMs) for the retrospective detection of exposure to NMs.

Nitrogen mustards (HN1, HN2 and HN3) are labile and rapidly degrade under certain environmental and biological conditions to give completely hydrolyzed products, *viz.* ethanolamines (EAs)[7] (Scheme S1, supporting information), which are less toxic than their parent compounds. Moreover, the presence of such hydrolyzed products in environmental and/or biomedical samples can provide valuable information about exposure to the parent compound. Because of the medicinal benefits of NMs, especially in cancer therapy, the corresponding amino alcohols have been extensively used to manufacture therapeutic cancer drugs/pro-drugs.[8] In addition, EAs can be used in the production of cosmetics.[9,10] Thus, these industries are subject to the CWC verification program conducted by the Organisation for the Prohibition of Chemical Weapons (OPCW).[2] During any OPCW inspection, non-compliance cannot be based on the identification of EAs, but the presence of partially hydrolyzed products of NMs, i.e. halfNMs, at those sites will support a non-compliance finding (Figure 1). Upon exposure to NMs, various adducts (e.g. DNA and protein adducts) and metabolites (e.g. partially and completely hydrolyzed products) are formed. Therefore, any biological samples collected from the victims of exposure to NMs are likely to contain the halfNMs. Thus, isolation and identification of halfNMs will provide significant evidence for the exposure of individuals to NMs.

HalfNMs are not amenable to analysis by gas chromatography (GC) because of the presence of polar hydroxyl groups and hence they have to be derivatized prior to GC/MS analysis. In a previous article GC/MS-based identification of halfNMs after derivatization by silylation was reported.[11] However, silylation of halfNMs has disadvantages: a long derivatization time, a high derivatization temperature, and a chromatogram with significant background peaks. These problems can be overcome by substituting derivatization by perfluoroacylation. Herein, we report on the advantages of perfluoroacylation for the sensitive and selective detection of halfNMs using electron ionization mass spectrometry (EI-MS) and positive chemical ionization mass spectrometry mass spectrometry (PCI-MS). Tandem mass spectrometry (MS/MS; precursor ion, product ion and neutral loss spectra) was also helpful in determining the fragmentation pathways. Furthermore, understanding the fragmentation pathways will help in selecting appropriate diagnostic precursor-to-product ion transitions for the selected reaction monitoring (SRM)/multiple reaction monitoring (MRM) detection of the target analytes in trace amounts in complex matrices.

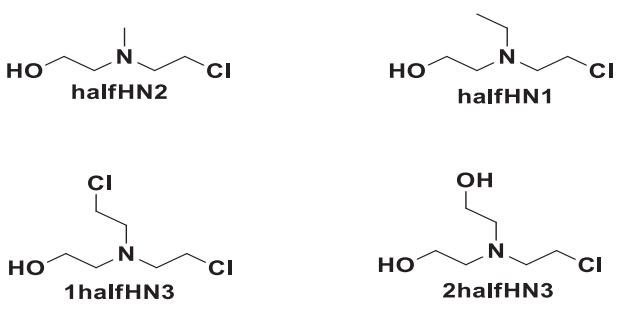

FIGURE 1 Chemical structures of different partially hydrolyzed products of NMs (halfNMs)

2 | EXPERIMENTAL

2.1 | Chemicals

Dichloromethane (DCM), acetone, and acetonitrile (ACN) were obtained from Merck (Mumbai, India) and *N*,*O*-bis(trimethylsilyl) trifluoroacetamide (BSTFA), *N*-methyl-*N*-*tert*-butyldimethylsilyltrifluoroacetamide (MTBSTFA), *N*-(trifluoroacetyl) imidazole (TFAI), *N*-(heptafluorobutyryl)imidazole (HFBI), *N*-methyldiethanolamine, *N*-ethyldiethanolamine, and triethanolamine were obtained from Sigma–Aldrich (Mumbai, India). Protonated salts of bis(2-chloroethyl) ethylamine [HN1], bis(2-chloroethyl) methylamine [HN2] and tris(2-chloroethyl)amine [HN3] were synthesized in microgram quantities in our laboratory when required and used immediately.

2.1.1 | Precautions

Nitrogen mustards are DNA alkylating and blister agents. These chemicals should be handled by trained professionals in an efficient fume hood equipped with an alkali scrubber and appropriate protective gear must be worn. A decontamination solution must be kept at the workplace and the solvent waste must be properly decontaminated.

2.2 | Instrumentation

GC/EI-MS studies were performed using a 6890N gas chromatograph coupled to a 5975B single quadrupole mass spectrometer controlled by Chemstation software (all supplied by Agilent Technologies, Santa Clara, CA, USA). A Trace 1300 gas chromatograph coupled to a TSQ Duo triple quadrupole mass spectrometer controlled by Xcalibur software (all supplied by Thermo Fisher Scientific, Waltham, MA, USA) was used for the EI-MS/MS, PCI-MS and MS/MS studies.

2.3 | GC/MS analysis

The transfer-line and injector temperatures were 280°C and 250°C, respectively. Helium was used as the carrier gas at a flow rate of 1 mL min^{-1}. A DB-5MS capillary column (30 m × 0.25 mm I.D., 0.25 μm film thickness; Thermo Fisher Scientific) was used for the separation. The GC oven temperature was programmed from 50°C (1 min hold) to 120°C at 40°C min^{-1}, raised to 161°C at 5°C min^{-1}, and finally to 280°C at 60°C min^{-1} (3 min hold). The scan range was from *m/z* 50 to 800 at a rate of 3.47 scans per second. GC/MS/MS analysis was carried out using the triple quadrupole instrument fitted with a CI source operating in positive ion multiple reaction monitoring (MRM) mode. MRM confirmation of each compound involved the use of two MRM transitions: the quantifier transition (Q) and the qualifier transition (q).

2.4 | Synthesis of partially hydrolyzed products of nitrogen mustards

The halfNMs were synthesized using our previously reported method[11] with some modification. Briefly, 1 mg of the salt of the NMs was dissolved in 1 mL of acetone/water (2:1 v/v) and incubated at room temperature with vigorous stirring. To this, an equimolar amount of 1 mM NaOH aqueous solution was added and the solution was stirred for 2 h. The evaporation of the mixture under a gentle nitrogen stream resulted in a solid residue (≥90% yield).

2.5 | Perfluoroacylation of halfNMs

Two different perfluoro-acyl derivatizing agents were used for derivatization: TFAI for trifluoroacetylation (TFA) and HFBI for heptafluorobutyrylation (HFB). The derivatizing agent (5 μL) was dissolved in 95 μL DCM, and to this 20 μg mL^{-1} of a mixed standard solution of halfNMs was added. After 5 min of incubation, a 1 μL sample from the DCM layer was subjected to GC/MS analysis.

[In the remainder of this article, the trifluoroacetyl derivatives of the halfNMs are abbreviated as halfHN2TFA, halfHN1TFA, 1halfHN3TFA and 2halfHN3TFA, and the heptafluorobutyryl derivatives as halfHN2HFB, halfHN1HFB, 1halfHN3HFB and 2halfHN3HFB, of the corresponding NMs.]

3 | RESULTS AND DISCUSSION

3.1 | Synthesis of halfNMs

The selective synthesis of halfNMs is challenging as the hydrolysis of NMs often yields the fully hydrolyzed products. Therefore, in our previous study[11] a controlled hydrolysis process was developed to yield the partial hydrolysis product. The protonated NMs (**I**) are highly soluble in water and remain in equilibrium with the free form (**II**) (Scheme S1, supporting information). In pure water, this equilibrium is shifted towards **I** due to their polar nature, making the rate of hydrolysis of **I** too slow. With the addition of acetone to the water, the free NMs becomes solubilized and the equilibrium shifts towards the free form (**II**), as shown in Scheme S1 (supporting information). Once the free form **II** is produced it undergoes partial hydrolysis *via* a reactive azeridinium intermediate (**III**). As the reaction progresses, the released HCl slows down the partial hydrolysis and it thus takes more than 20 h to obtain the desired halfNMs (**IV**). To speed up the reaction, stoichiometric amounts of very dilute (1 mM) NaOH solution were added, which consumes the released HCl, and the desired product was obtained within 2 h. The progress of the reaction was monitored by GC/MS after derivatizing the halfNMs with HFBI.

3.2 | Selection of perfluoroacylation over silylation

The halfNMs (halfHN1, halfHN2, 1halfHN3 and 2halfHN3) were monitored by GC/EI-MS after derivatization by four different derivatizing agents (BSTFA, MTBSTFA, TFAI and HFBI, as shown in Scheme 1). High temperature (>70°C) is required for silylation and at this elevated temperature degradation of the silylating agents occurs. The degradation products or byproducts[12] produced during the

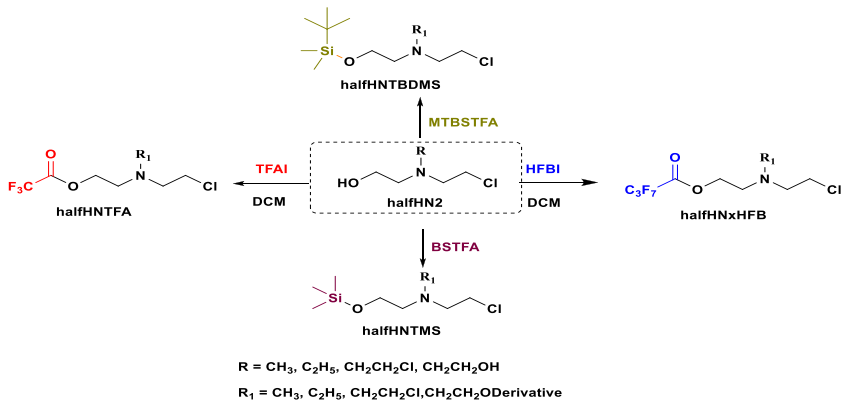

SCHEME 1 Derivatives of partially hydrolyzed products of NMs (TMS, TBDMS, TFA and HFB) [Color figure can be viewed at wileyonlinelibrary.com]

derivatization create a high GC background and mask the analytes, especially the early eluting compounds, as shown in Figures 2A and 2B. It is clear from Figure 2 that the halfHN1TBDMS derivative is heavily masked by the degradation products/byproducts generated by the MTBSTFA. Several additional peaks can be seen (Figure 2) in the total ion chromatogram (TIC) of the TMS and TBDMS derivatives while using pure analytes at higher concentration than with the TFA or HFB derivatives. On the other hand, trifluoroacetylation and heptafluorobutyrylation occur at room temperature and a clean chromatogram is obtained, as shown in Figures 2C and 2D. Thus, this reduction in background noise enhances the sensitivity.

The derivatization of halfNMs using perfluoroacylation is almost instantaneous, whereas the silylation reaction takes at least 30 min for complete derivatization. Thus, the reduction in derivatization time is very useful for high-throughput sample analysis.

Moreover, the molecular ion and abundant high-mass fragment ions were observed in the mass spectra of the perfluoroacyl derivatives of halfNMs, whereas the corresponding silyl derivatives provided abundant fragment ions at low *m/z* values only. The presence of the molecular ion and the high-mass fragment ions for the perfluoroacyl derivatives improves the selectivity of the detection. In addition, these abundant high-mass ions open the opportunity to develop a MS/MS method for the detection of these analytes at trace level. For the TMS or TBDMS derivatives the abundance for most of the fragment ions was less than 30% of the base peak, whereas, for the TFA and HFB derivatives, two or more ions have an abundance of ≥50% of the base peak. Hence, the perfluoroacyl derivatives are also useful for the identification of these compounds in complex matrices using extracted ion chromatograms.

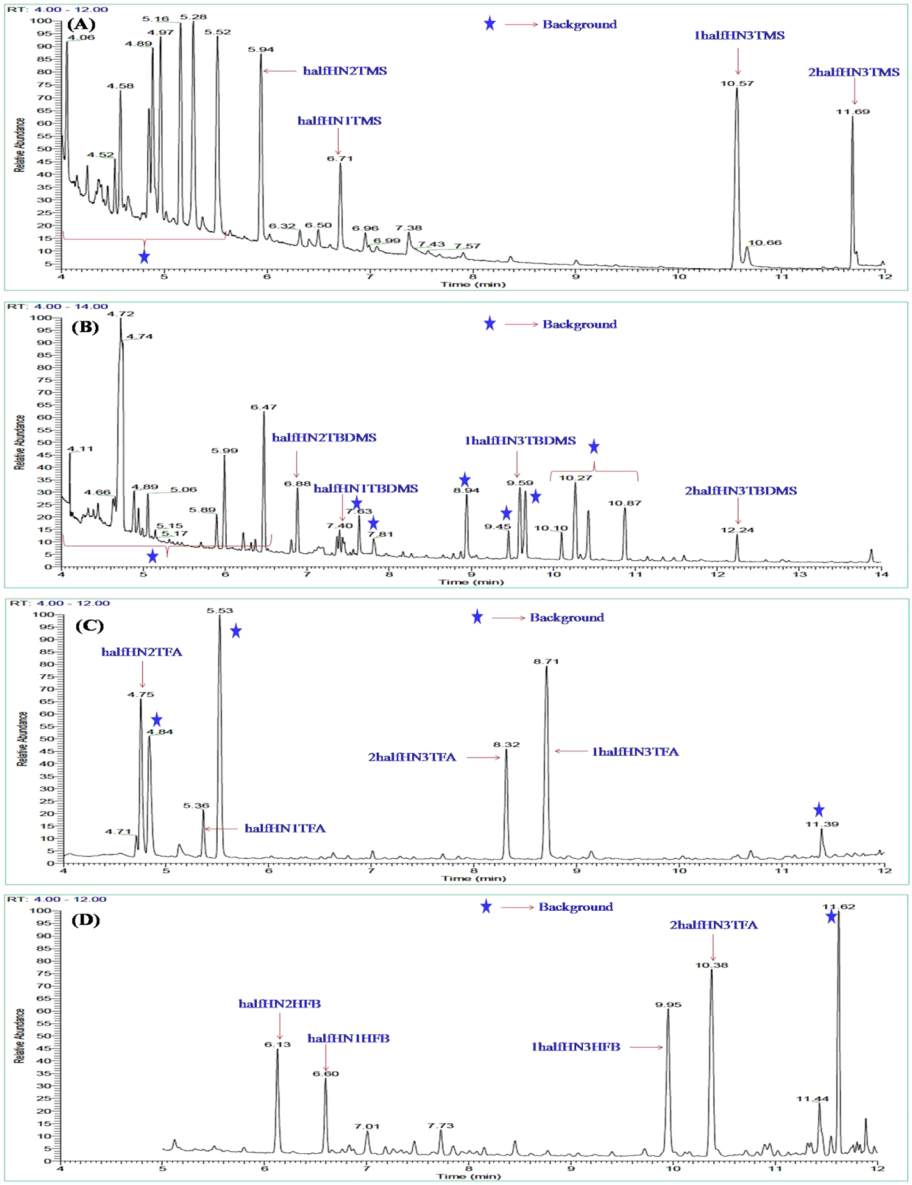

FIGURE 2 Total ion chromatograms obtained during GC/EI-MS analysis of A, TMS; B, TBDMS; C, TFA; and D, HFB derivatives of halfNMs [Color figure can be viewed at wileyonlinelibrary.com]

TABLE 1 EI-MS data of TFA derivatives of halfHNs

R'	Compound	RI*	$M^{\bullet+}$	Fragment ions (% of relative abundance)								
				(1)	(2)	(3)	(4)	(5)	(6)	(7)	(8)	(9)
Me	HalfHN2TFA	1116	233	106 (99.9)	184 (88.7)	141 (50.5)	198 (8.6)	120 (8.9)	92 (2.3)	63 (26.7)	56 (9.4)	69 (43.3)
Et	halfHN1TFA	1160	247	120 (93.5)	198 (99.9)	141 (52.6)	212 (9.9)	134 (7.6)	92 (14.0)	63 (21.9)	56 (44.0)	-
CH_2CH_2Cl	1halfHN3TFA	1396	281	154 (43.4)	232 (99.9)	141 (60.4)	246 (6.4)	168 (3.6)	92 (10.3)	63 (47.6)	56 (29)	69 (32.2)
$CH_2CH_2OSiMe_3$	2halfHN3TFA	1368	359	232 (68.6)	310 (48.7)	141 (99.9)	324 (4.0)	246 (6.2)	92 (3.1)	63 (24.1)	56 (20.2)	69 (54.0)

*Retention index.
For ions (**1**)–(**5**) see Scheme 2, for ion (**6**) see Scheme S5 (supporting information), for ions (**7**)–(**9**) see Scheme S6 (supporting information).

TABLE 2 EI-MS data of HFB derivatives of halfNMs

R'	Compounds	RI*	$M^{\bullet+}$	Fragment ions (% of relative abundance)							
				(1)	(2)	(3)	(4)	(5)	(6)	(7)	(8)
Me	halfHN2HFB	1156	333	106 (99.9)	284 (80.1)	241 (23.0)	298 (7.5)	120 (16.8)	92 (3.1)	63 (22.3)	56 (8.3)
Et	halfHN1HFB	1204	347	120 (86.2)	298 (99.9)	241 (28.0)	312 (9.2)	134 (13.4)	92 (9.5)	63 (14.2)	56 (26.8)
CH_2CH_2Cl	1halfHN3HFB	1456	381	154 (56.3)	332 (99.9)	241 (41.2)	346 (6.7)	168 (10.6)	92 (12.5)	63 (68.2)	56 (41.0)
$CH_2CH_2OOC_3F_7$	2halfHN3HFB	1471	559	332 (99.9)	510 (40.9)	241 (86.3)	524 (3.0)	346 (30.0)	92 (4.5)	63 (28.7)	56 (29.2)

*Retention index.
For ions (**1**)–(**5**) see Scheme 2, for ion (**6**) see Scheme S5 (supporting information), for ions (**7**) and (**8**) see Scheme S6 (supporting information), for ion (**9**) see Scheme S7 (supporting information).
For ions (**10**) and (**11**) see Scheme S7 (supporting information), for ions (**A**)–(**C**) see Scheme S8 (supporting information).

TABLE 2 EI-MS data of HFB derivatives of halfNMs

R'	Fragment ions (% of relative abundance)								
	(9)	(10)	(11)	(12)	(13)	(14)	(15)	(A)	(B)	(C)
Me	69 (26.3)	169 (38.3)	100 (44.11)	84 (2.1)	223 (4.1)	213 (2.4)	197 (1.4)	-	-	-
Et	69 (21.6)	169 (30.9)	100 (3.9)	84 (10.2)	223 (2.8)	213 (1.8)	197 (1.3)	-	-	-
CH_2CH_2Cl	69 (36.5)	169 (46.0)	100 (5.8)	84 (2.5)	223 (2.8)	213 (2.8)	197 (1.5)	270 (4.3)	296 (<1)	118 (10.0)
$CH_2CH_2OOC_3F_7$	69 (57.3)	169 (84.7)	100 (29.2)	84 (1.9)	223 (2.9)	213 (5.4)	197 (3.3)	270 (7.3)	296 (3.2)	118 (7.7)

*Retention index.
For ions (**1**)–(**5**) see Scheme 2, for ion (**6**) see Scheme S5 (supporting information), for ions (**7**) and (**8**) see Scheme S6 (supporting information), for ion (**9**) see Scheme S7 (supporting information).
For ions (**10**) and (**11**) see Scheme S7 (supporting information), for ions (**A**)–(**C**) see Scheme S8 (supporting information).

3.3 | Retention indices

The retention indices of each derivatized compound were calculated, as shown in Table 1 for halfHNxTFA derivatives and Table 2 for halfHNxHFB derivatives (according to the Van Den Dool and Kartz formula[13]), to provide an additional degree of specificity for the detection and identification of targeted metabolites by EI-MS.

3.4 | Mass spectral fragmentation analysis of perfluoroacyl derivatives

3.4.1 | EI-MS interpretation

The fragmentation of the EI molecular ions involves two important fragmentation reactions: (a) α-homolytic cleavage and (b) inductive heterolytic cleavage. In the spectra of the halfHNxTFA ($M^{+\bullet}$ at *m/z* 233, 247, 281 and 359, for halfHN2TFA, halfHN1TFA, 1halfHN3TFA and 2halfHN3TFA, respectively) and halfHNxHFB ($M^{+\bullet}$ at *m/z* 333, 347, 381 and 559 for halfHN2HFB, halfHN1HFB, 1halfHN3HFB and 2halfHN3HFB, respectively) derivatives, series of even-electron fragment ions (EE^+) were observed. Most of the fragmentation pathways were common to all halfHNxTFA and halfHNxHFB derivatives, but they differed significantly from those of the respective silyl derivatives.

The mass spectra of the halfHNxHFB derivatives follow a similar fragmentation pathway to the halfHNxTFA compounds and also provide similar fragment ions, with differences in their masses due to the difference in the perfluoroalkyl group, i.e. CF_3 in TFA and C_3F_7 in HFB. The spectra of the perfluoroacyl derivatives of the halfNMs are similar to those of the corresponding EAs.[14–16] The EI mass spectra of all the derivatives of the halfNMs are shown in Figure 3 (3A – halfHN1TFA, 3B – halfHN2TFA, 3C – 1halfHN3TFA and 3D – 2halfHN3TFA) and Figure 4 (4A – halfHN1HFB, 4B – halfHN2HFB, 4C – 1halfHN3HFB and 4D – 2halfHN3HFB). The common fragmentation pathways and the corresponding fragment ions are depicted in Scheme 2. As a result of the α-cleavage, intense ions ($[M - R_2COOCH_2]^+$ (**1**) and $[M - 49]^+$ (**2**)) are formed, with the assumption that the radical cation is formed on the nitrogen atom (as shown in Scheme S2, supporting information). Ion (**1**) results from the elimination of a methyl perfluoroalkanoate radical (CF_3COOCH_2 for the TFA derivative and $C_3F_7COOCH_2$ for HFB) from the ester moiety side and ion (**2**) from the loss of a chloromethyl radical (49 u) from the 2-chloroethyl group, as depicted in Scheme 2. Another abundant ion resulted from the loss of $[R_1NCH_2CH_2Cl]$ (**3**) from the molecular ion (at *m/z* 141 for TFA and *m/z* 241 for HFB) by inductive cleavage at the C–N bond next to the ester group after the elimination of an amine radical (Scheme S3, supporting information).

When radical cation formation occurred on the chlorine atom, inductive cleavage led to the formation of a low-abundance $[M - 35]^+$ ion (**4**) by elimination of a chlorine atom (35 u) (Scheme S3, supporting information). When radical cation formation occurred on the oxygen atoms of the ester group, inductive cleavage yielded a low-abundance

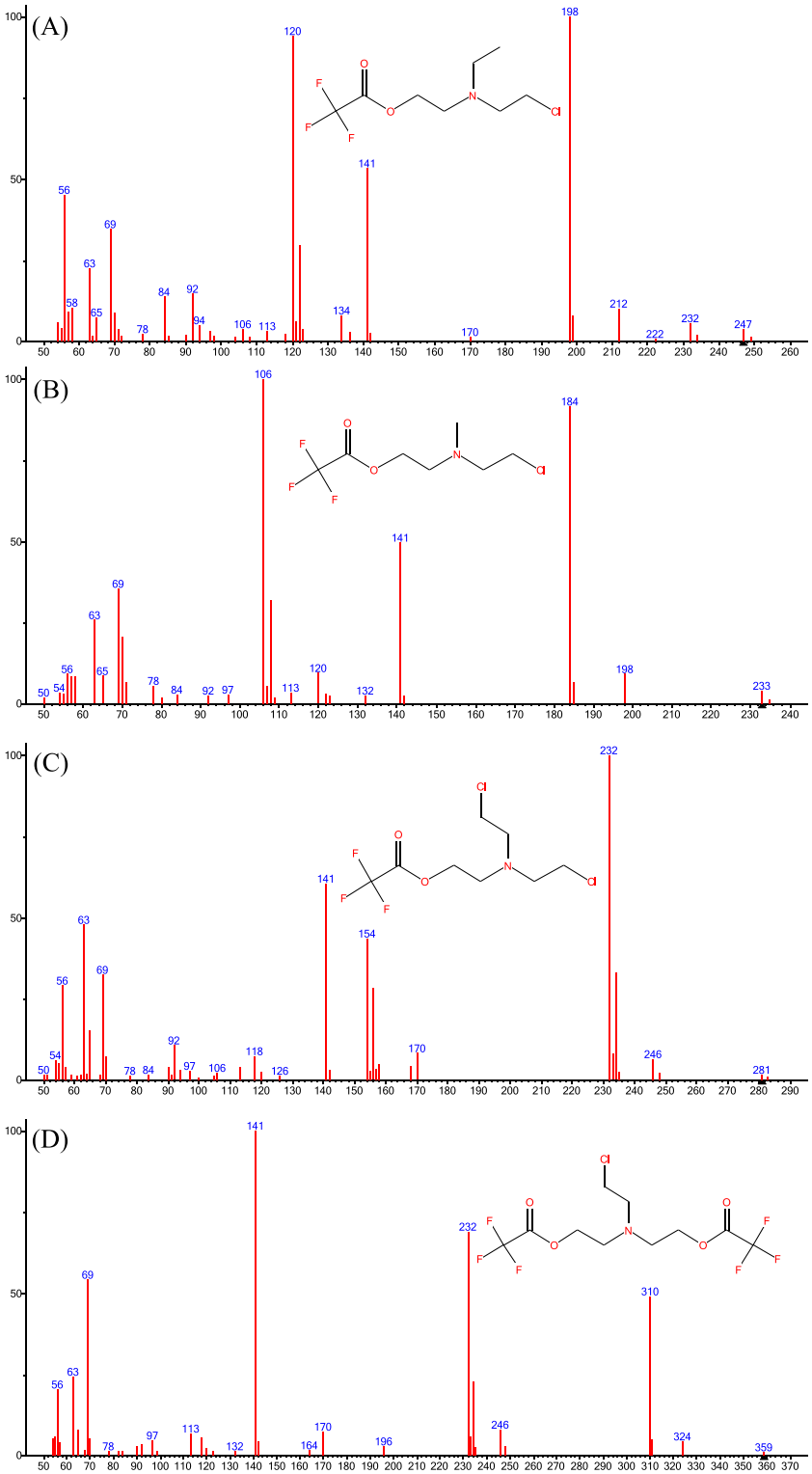

FIGURE 3 EI-MS spectra of A, halfHN1TFA; B, halfHN2TFA; C, 1halfHN3TFA; and D, 2halfHN3TFA [Color figure can be viewed at wileyonlinelibrary.com]

$[M - R_2COO]^+$ ion (**5**) after the elimination of the perfluoroalkanoate radical (CF_3COO from the TFA derivative and C_3F_7COO from HFB) (Scheme S3, supporting information).

Another characteristic ion (**6**) is formed at *m/z* 92, which results from the EE^+ fragment ion $[M - R_2COOCH_2]^+$ (this pathway is supported by the precursor ion scan of *m/z* 92 depicted in Figure S1D, supporting information) after βH-rearrangement[17] from the β carbon of the R_1 group to the N atom, as shown in Scheme S4 (supporting information). Inductive cleavage of the $[M - R_2COOCH_2]^+$ ion at the C–N bond provides a characteristic ion at *m/z* 63 (**7**) ($^+CH_2CH_2Cl$) after expulsion of a neutral imine. A precursor ion scan of *m/z* 63 (Figure S1B, supporting information) shows that this ion can also arise from *m/z* 92 and 134, i.e. from ions containing the $-CH_2CH_2Cl$ group. A three-membered cyclic

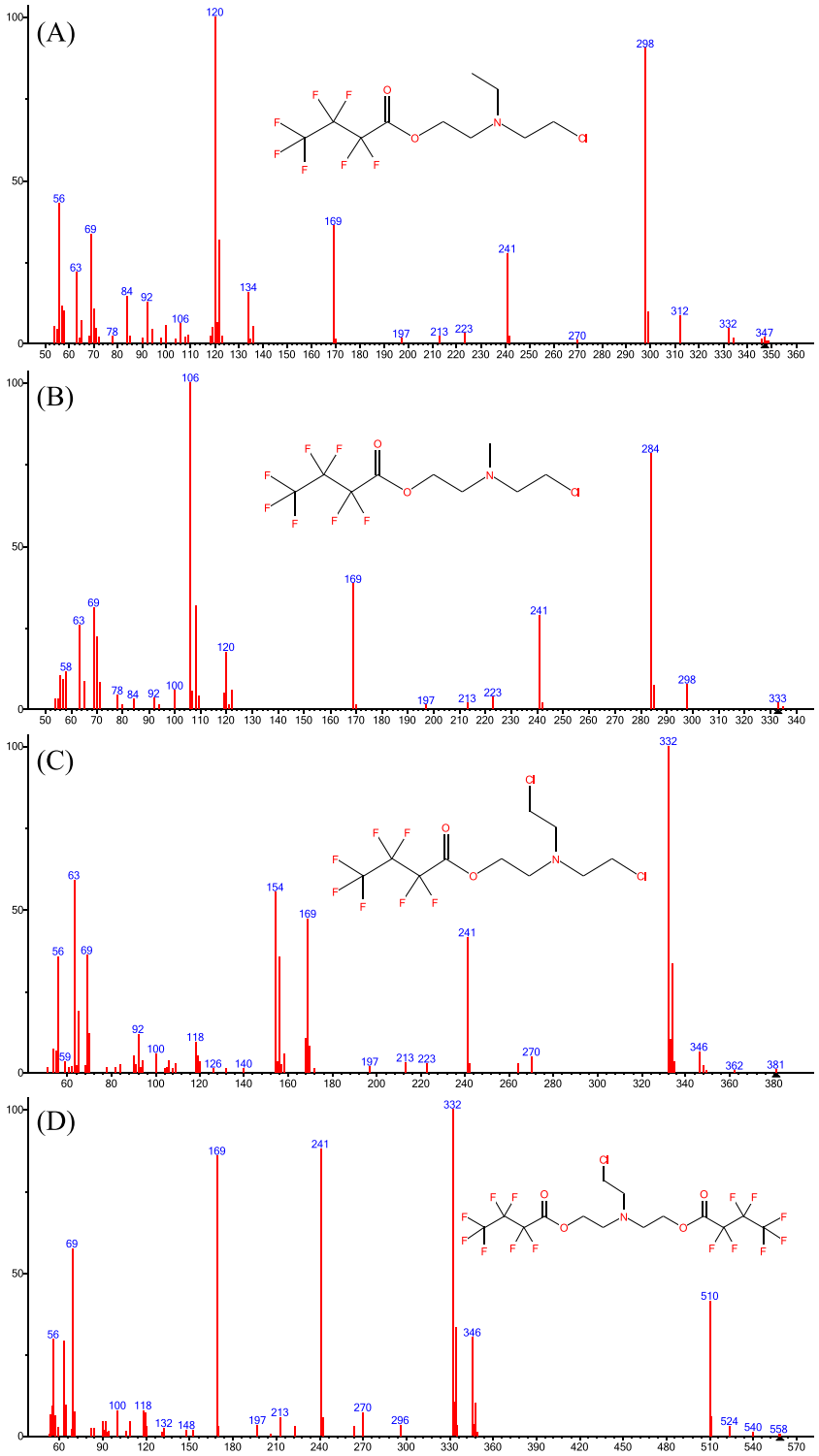

FIGURE 4 EI-MS spectra of A, halfHN1HFB; B, halfHN2 HFB; C, 1halfHN3 HFB; and D, 2halfHN3 HFB [Color figure can be viewed at wileyonlinelibrary.com]

N-methylene aziridinium ion is produced at *m/z* 56 (**8**) which can result from any of the nitrogen-containing intermediate ions such as (**1**), (**2**), (**4**), (**5**) and (**6**), as depicted in Scheme S5 (supporting information), and this pathway is supported by the precursor ion scan of *m/z* 56 (Figure S1A, supporting information).

A moderately abundant peak observed at *m/z* 69 (**9**) corresponds to the trifluoromethyl cation, resulting from C–C bond cleavage in the perfluoroalkyl chain. A precursor ion scan of this ion (Figure S1C, supporting information) confirms that it arises from intermediate ions containing the perfluoroalkyl moiety (Scheme S6, supporting information), such as *m/z* 97 (R_2CO^+), 113 (R_2COO^+), 141 ($R_2COOCH_2CH_2^+$), and $[M - 35]^+$ and $[M - 49]^+$. The HFB derivative yields two additional ions, at *m/z* 169 and 100, that result from the heptafluorobutyl cation and the 1,1,2,2-tetrafluoroethylene radical cation, respectively, by loss of the trifluoromethyl radical, as depicted in Scheme S7 (supporting information).

SCHEME 2 Common fragmentation pathways in EI-MS spectra for HFB and TFA derivatives of partially hydrolyzed products of HNs

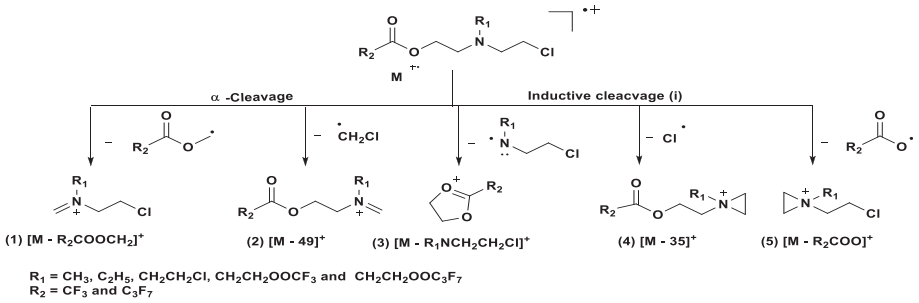

The perfluoroacyl derivatives of the partially hydrolyzed products of HN3 show some additional fragment ions formed through H-rearrangement and βH-elimination: (**A**) $[M - C_2H_3Cl]^+$ (at *m/z* 170 or 270), (**B**) $[M - HX]^+$ (at *m/z* 196 or 296) and (**C**) $[M - R_2COOH]^+$ (at *m/z* 118), as shown in Scheme S8 (supporting information). In halfHN3 the expulsion of a chloromethyl radical from $M^{+\bullet}$ via α-cleavage resulted in the $[M - 49]^+$ ion (**2**) (at *m/z* 232 and 310, or *m/z* 332 and 510, respectively, for the TFA and HFB derivatives). This ion can be further fragmented to give ions (**A**), (**B**) and (**C**). Ion (**A**) was produced after the elimination of a vinyl chloride radical *via* H-rearrangement from the β-C to N. Ion (**B**) was formed by loss of HX (X can be the heteroatom (Cl) or the perfluoroacyl group) *via* a βH-elimination. Similarly, ion (**C**) is formed after the loss of the perfluoroacyloic acid (trifluoroacetic acid or heptafluorobutyric acid), as depicted in Scheme S9 (supporting information).

3.4.2 | Interpretation of CI-MS spectra

As was observed in the EI-MS spectra, the PCI-MS spectra of the TFA and HFB derivatives of halfNMs are similar. We report herein only on the TFA derivatives, since both derivatives follow similar fragmentation pathways. The fragment ion observed in PCI-MS for halfHN1TFA ($[M + H]^+$ at *m/z* 248), halfHN2TFA ($[M + H]^+$ at *m/z* 234), 1halfHN3TFA ($[M + H]^+$ at *m/z* 282), and 2halfHN3 ($[M + H]^+$ at *m/z* 360) are shown in Figures S2A, S2B, S2C and S2D (supporting information), respectively. Each $[M + H]^+$ ion (**C1**) follows a unique fragmentation pattern in PCI. The $[M + H]^+$ ions provide fragment ions (**C2**) at $[M + H - HF]^+$, (**C3**) at $[M + H - HCl]^+$ and (**C4**) $[M + H - CH_3Cl]^+$ for all the TFA derivatives of halfNMs (Figure S2, supporting information). Another fragment ion (**C5**) $[M + H - CF_3COOH]^+$ is obtained for each molecule (except halfHN1TFA), as depicted in Figures S2B, S2C and S2D (supporting information). All the fragment ions are summarized in Scheme 3. During the PCI-MS/MS or MS/MS analysis of the protonated molecule a wide range of fragmentation reactions was observed (Figure 4). Collision-induced dissociation (CID) fragmentation of the $[M + H]^+$ ion occurs either *via* inductive cleavage of the C–heteroatom (N, O, Cl, etc.) bond with charge migration to the α-C-atom, as shown in Scheme S10 (supporting information), or via a four-centered H-rearrangement (acyclic EE^+ cleavage) with charge retention on the heteroatom as depicted in Scheme S11 (supporting information). The MS/MS fragmentation pathways were investigated using 1halfHN3TFA as an example (Figure S3A, supporting information). The protonated molecule (**1**) at *m/z* 282 (Figure S3B, supporting information) provides eight (**C5** to **C12**) product ions (Scheme 4). When protonation occurs on the N atom, the inductive cleavage fragmentation follows two pathways, path-a and path-b, as depicted in Scheme S10 (supporting information). Path-a gives the most abundant product ion (**C9**) at *m/z* 141 generated after the neutral loss of the secondary amine ($ClCH_2CH_2NHCH_2CH_2Cl$). Ion (**C9**) then undergoes another inductive cleavage by the expulsion of an ethylene molecule to provide the

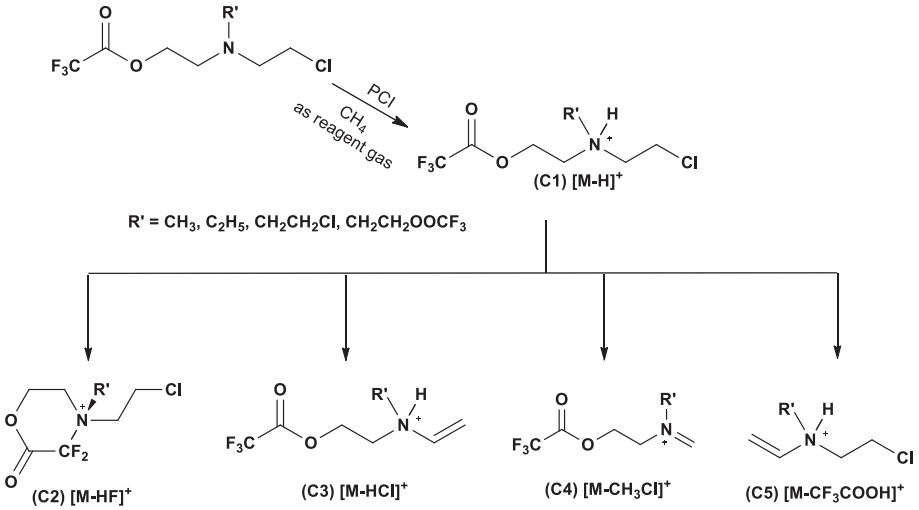

SCHEME 3 PCI-MS fragmentation pathways of the TFA derivatives of halfNMs

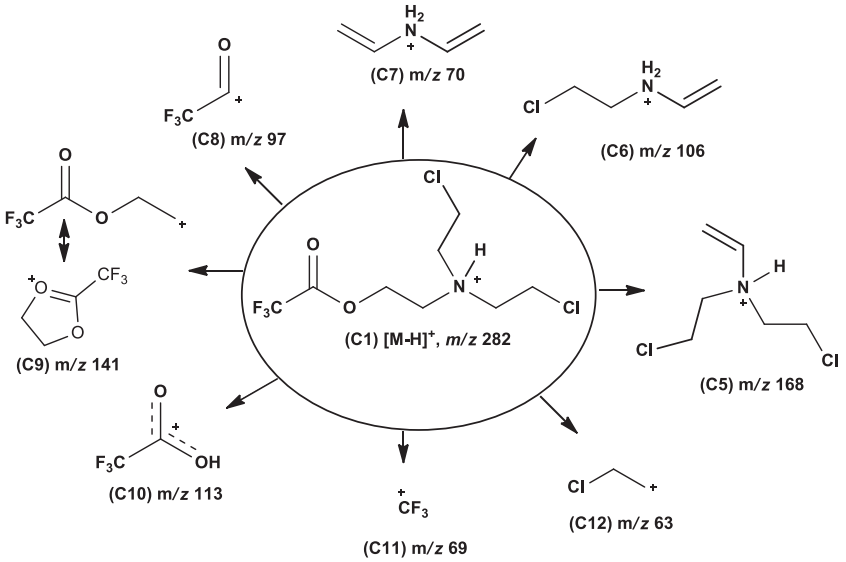

SCHEME 4 Different product ions of the protonated molecule of 1halfHN3TFA after MS^2

trifluoroacetate cation (CF_3COO^+) (**C10**) at *m/z* 113. Neutral loss of CO_2 from *m/z* 113 gives an intense CF_3^+ ion (**C11**) at *m/z* 69.

Path-b provides the characteristic 2-chloroethyl cation (**C12**) at *m/z* 63 after the expulsion of the secondary amine (Scheme S10, supporting information). If protonation occurs at the alkoxy oxygen atom of the ester linkage, after C–O bond cleavage charge migration occurs on the carbonyl C to form the trifluoroacetyl cation (**C8**) at *m/z* 97 (Scheme S10, supporting information). Cleavage at the alkoxy O–C bond of the ester moiety in the protonated molecule (**C1**) by β-elimination releases trifluoroacetic acid to yield a product ion (**C5**) at *m/z* 168 (Scheme S11, supporting information). This ion can then eliminate vinyl chloride by H-rearrangement to give the product ion (**C6**) at *m/z* 106. Final β-elimination of HCl from (**C6**) provides the characteristic di-vinyl ammonium ion (**C7**) (Scheme S11, supporting information) at *m/z* 70.

4 | CONCLUSIONS

To the best of our knowledge, this is the first report of the mass spectral study of perfluoroacyl derivatives of half nitrogen mustards. The unequivocal identification of halfNMs was demonstrated by GC/MS/MS analysis after perfluoroacyl derivatization. The proposed fragmentation pathways are supported by precursor ion scanning of crucial product ions. Most of the product ions obtained in the PCI-MS/MS spectra of protonated molecules were similar to the fragment ions obtained in the EI-MS spectra. The combination of these mass spectral techniques added an extra dimension to the identification of unknown compounds. Moreover, the two types of perfluoroacylated derivatives generated complementary GC/EI-MS, GC/EI-MS/MS, GC/PCI-MS and GC/PCI-MS/MS data which helps in the identification of unknown metabolites in a fast and reliable fashion.

ACKNOWLEDGEMENTS

The authors thank DRDE, Gwalior, and DRDO, New Delhi, for funding and fellowship. They also thank Dr D.K. Dubey, Director, DRDE, Gwalior, for his keen interest and encouragement, and all their colleagues and lab mates for their unconditional support. This manuscript is assigned DRDE accession no. DRDE/VTX/42/2019.

ORCID

Meehir Palit https://orcid.org/0000-0003-0648-239X

REFERENCES

1. Chauhan S, D'cruz R, Faruqi S, et al. Chemical warfare agents. *Environ Toxicol Pharmacol*. 2008;26(2):113-122.
2. FOLLOWS HAA. *Convention on the prohibition of the development, production, stockpiling and use of chemical weapons and on their destruction*. The Hague: The Netherlands; 2005.
3. Willison SA. Wipe selection for the analysis of surface materials containing chemical warfare agent nitrogen mustard degradation products by ultra-high pressure liquid chromatography–tandem mass spectrometry. *J Chromatogr A*. 2012;1270:72-79.
4. Osborne MR, Wilman DE, Lawley PD. Alkylation of DNA by the nitrogen mustard bis(2-chloroethyl) methylamine. *Chem Res Toxicol*. 1995;8(2):316-320.
5. Thompson VR, DeCaprio AP. Covalent adduction of nitrogen mustards to model protein nucleophiles. *Chem Res Toxicol*. 2013;26(8):1263-1271.
6. Golime R, Chandra B, Palit M, Dubey D. Adductomics: A promising tool for the verification of chemical warfare agents' exposures in biological samples. *Arch Toxicol*. 2019;93(6):1473-1484.
7. Otsuka M, Miyaguchi H, Uchiyama M. Analysis of degradation products of nitrogen mustards via hydrophilic interaction liquid chromatography–tandem mass spectrometry. *J Chromatogr A*. 1602; 2019:199-205.
8. Kuang Y, Balakrishnan K, Gandhi V, Peng X. Hydrogen peroxide inducible DNA cross-linking agents: Targeted anticancer prodrugs. *J Am Chem Soc*. 2011;133(48):19278-19281.
9. Fiume MM, Heldreth B, Bergfeld WF, et al. Safety assessment of triethanolamine and triethanolamine-containing ingredients as used in cosmetics. *Int J Toxicol*. 2013;32(3_suppl):59S-83S.

10. Lessmann H, Uter W, Schnuch A, Geier J. Skin sensitizing properties of the ethanolamines mono-, di-, and triethanolamine. Data analysis of a multicentre surveillance network (IVDK*) and review of the literature. *Contact Dermatitis*. 2009;60(5):243-255.
11. Chandra B, Sinha Roy K, Shaik M, Waghmare C, Palit M. Mass spectral studies of silyl derivatives of partially hydrolyzed products of nitrogen mustards: Important markers of nitrogen mustards exposure. *Rapid Commun Mass Spectrom*. 2020;34:e8586.
12. Soni NR. Improve GC separations with derivatization for selective response and detection in novel matrices. *J Environ Life Sci*. 2016;1(1): 14-25.
13. van Den Dool H, Kratz PD. A generalization of the retention index system including linear temperature programmed gas—liquid partition chromatography. *J Chromatogr A*. 1963;11:463-471.
14. Palit M, Mallard G. Dispersive derivatization liquid–liquid extraction of degradation products/precursors of mustards and V-agents from aqueous samples. *J Chromatogr A*. 2011;1218(32): 5393-5400.
15. Pardasani D, Palit M, Gupta A, Kanaujia PK, Dubey D. Gas chromatography–mass spectrometry analysis of trifluoroacetyl derivatives of precursors of nitrogen and sulfur mustards for verification of chemical weapons convention. *J Chromatogr A*. 2004; 1059(1–2):157-164.
16. Saeidian H, Sarabadani M, Babri M. Electron ionization mass spectral studies of phenoxide derivatives of mustards: Implications for analysis to support chemical weapons convention. *Int J Mass Spectrom*. 2015;383:1-12.
17. Niessen WM, Correa C RAC. *Interpretation of MS-MS Mass Spectra of Drugs and Pesticides*. Wiley Series on Mass Spectrometry no. 51. Hoboken, NJ: John Wiley & Sons, Inc.; 2017.

SUPPORTING INFORMATION

Additional supporting information may be found online in the Supporting Information section at the end of this article.

How to cite this article: Chandra B, Sinha Roy K, Shaik M, Waghmare C, Palit M. Mass spectral fragmentation of perfluoroacyl derivatives of half nitrogen mustards for their detection by gas chromatography/mass spectrometry. *Rapid Commun Mass Spectrom*. 2020;34:e8777. https://doi.org/10.1002/rcm.8777